

S. B. Samavedam, H. H. Tseng, P. J. Tobin, J. Mogab, S. Dakshina-Murthy*, L. B. La, J. Smith, J. Schaeffer, M. Zavala, R. Martin, B.-Y. Nguyen, L. Hebert, O. Adetutu, V. Dhandapani, T.-Y. Luo, R. Garcia, P. Abramowitz, M. Moosa, D. C. Gilmer, C. Hobbs, W. J. Taylor, J. M. Grant, R. Hegde, S. Bagchi, E. Luckowski, V. Arunachalam, M. Azrak.
Digital DNA Laboratories, 3501 Ed Bluestein Blvd., MD:K10, (*AMD)
Austin, TX 78721, USA. (Tel: 512-933-7180, FAX: 512-933-8787, sri.samavedam@motorola.com)

Abstract

We report for the first time electrical characterization of HfO₂ p- and n-MOSFETs with CVD TiN and PVD TaSiN gates respectively fabricated using conventional CMOS integration. Their performance is compared to PVD TiN-gated HfO₂ and SiO₂ n- and p-MOSFETs. To understand the issues with metal gates on high K gate dielectrics, PVD TiN MOSFETs were extensively characterized. At 10nA/μm leakage, 0.345mA/μm drive current was obtained from PVD TiN/HfO₂ p-MOSFETs. HfO₂ n-MOSFETs with metal gates show about 10⁴ times reduction in gate leakage compared to poly/SiO₂ devices.

Introduction

The decrease in the inversion capacitance due to depletion in polysilicon (poly) gates will be significant as the gate dielectric is scaled below 10Å equivalent oxide thickness (EOT). Metal gates will eliminate gate depletion and address other issues like boron penetration and increased gate resistance, which will be aggravated as the poly gate thickness is scaled down. Extensive simulations have shown that the optimal gate work-function for sub-50 nm gate lengths is 0.2 eV below (above) the conduction (valence) band edge of silicon for NMOS (PMOS) [1]. Recently, PVD Ta_xSi_yN (TaSiN) has been reported to be an NMOS-compatible metal gate [2,3]. CVD TiN on HfO₂ has a work-function of 4.8eV, suitable for a PMOS gate. We report for the first time electrical characterization of HfO₂ n-MOSFETs with PVD TaSiN gates and p-MOSFETs with CVD TiN gates. PVD TiN-gated HfO₂ and SiO₂ n- and p-MOSFETs were used for comparison and understanding the difference between metal gates on SiO₂ versus HfO₂.

Experiment

Metal gate MOSFETs were processed using a 0.13μm CMOS technology [4]. The HfO₂ gate dielectric was deposited by MOCVD at 550°C. PVD TaSiN and PVD TiN gates were reactively sputtered. CVD TiN was deposited using Tetrakis-dimethylamino-titanium at 450° C. SiO₂ devices with PVD TiN gates were used as controls.

Results and Discussion

A. Work-function and thermal stability

TEM studies (Fig. 1) indicate that PVD TaSiN films on HfO₂ remain amorphous after a high temperature anneal unlike TiN (PVD and CVD) gates. The absence of grain boundary diffusion minimizes reaction at the TaSiN/HfO₂ interface. However, post-gate annealing increases the CETacc (capacitance equivalent thickness under accumulation) of TaSiN/HfO₂ MOSCAPs more than PVD or CVD TiN/HfO₂ (Fig. 2). The work-functions of PVD TaSiN and CVD TiN on HfO₂ were determined to be 4.4eV and 4.8eV which makes them suitable candidates for NMOS and PMOS respectively. Post-gate annealing can change the V_{fb}, fixed charge and work-function in metal-gated HfO₂ devices.

B. Transistor characterization

Figs. 3 and 4 show typical high frequency CVs from HfO₂ p- and n-MOSFETs with different metal gates. Note the absence of gate depletion (C_{inv}/C_{acc}~1) as expected. The kink in the TaSiN/HfO₂ devices is suggestive of the interface defect state recently identified in HfO₂ MOSCAPs [5]. Fig. 5 shows well-behaved Id-Vd

characteristics of 10μm x 10μm (W/L) HfO₂ p- and n-MOSFETs with CVD TiN and TaSiN gates respectively. Fig. 6 shows the sub-threshold characteristics of long channel n- and p-MOSFETs with different metal gates. PVD and CVD TiN-gated devices show excellent sub-threshold swings of ~70mV/dec. The poor sub-threshold behavior of TaSiN/HfO₂ n-MOSFETs suggests a high interface state density consistent with the existence of a kink in CVs (Fig. 4).

Fig. 7 shows HfO₂ PMOS Ion/Ioff characteristics with a PVD TiN gate. At 10nA/μm leakage, drive current is 0.375mA/μm. Short-channel n-MOSFETs with metal gates has a steep V_t roll-off and hence degraded Ion/Ioff characteristics at 10nA/μm leakage. Controlling V_t roll-off at sub-90nm gate lengths when metal gate work-functions are displaced from the band-edges requires optimization of channel and halo doping and thermal budget. Fig. 8 shows nmos and pmos linear G_m normalized to V_t and CETinv (capacitance equivalent thickness under inversion) to compare electron and hole mobilities. The peak electron (hole) mobility for HfO₂ devices is 39%-48% (27%-48%) lower compared to SiO₂ devices at comparable channel doping.

C. Gate leakage and reliability

Fig. 9 shows the gate leakage in n-MOSFETs at V_t+1V as a function of CETinv. PVD TiN and TaSiN-gated HfO₂ devices show about 10⁴X reduction in gate leakage compared to poly/SiO₂ devices at comparable inversion capacitance. Fig. 10 shows a similar plot for PMOS. Higher charge pumping current in HfO₂ devices compared to SiO₂ devices with PVD TiN gates suggests ~4X higher interface trap density (Fig. 11). Fig. 12 shows variation in V_t and G_m with time under 7.6 MV/cm (V_g=-1.3V, CETinv~17Å) stressing in PVD TiN/HfO₂ p-MOSFETs. A -100mV shift in V_t and peak G_m was observed due to charge trapping after 100s, which remains unchanged up to 1000s. Fig. 13 shows 105° C TDDB (time-dependent dielectric breakdown) data from PVD TiN/HfO₂ p-MOSFETs suggesting that these devices are capable of reasonably high operating voltages to meet a 10-year lifetime criterion.

Conclusion

We have successfully fabricated and characterized HfO₂ n-MOSFETs with TaSiN and PVD TiN gates and p-MOSFETs with CVD and PVD TiN gates using a conventional CMOS process. Metal-gated HfO₂ n-MOSFETs show a 10⁴X gate leakage reduction compared to poly/SiO₂ devices. Reasonable Ion/Ioff performance and reliability were observed in PVD TiN/HfO₂ PMOS. CET and work-function variation with thermal budget, mobility degradation, V_t roll-off control and charge trapping are key issues that need to be addressed with metal gates on high-K gate dielectrics. Identification of optimum metal gate materials and processes requires further study.

References

- [1] B. Cheng et al. 2001 IEEE Intl. SOI Symp. Proc., pp. 91-92, 2001.
- [2] Y.-S. Suh et al. VLSI Tech Digest, pp. 47-48, 2001.
- [3] D.-G. Park et al. IEDM Tech Digest, pp. 671-74, 2001.
- [4] A. H. Perera et al. IEDM Tech Digest, pp. 571-74, 2000.
- [5] S. Mudanai et al. Unpublished, 2001.

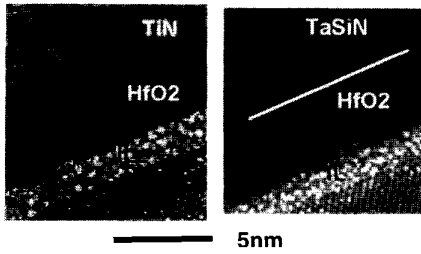


Fig. 1 Cross-section TEM images of TiN/HfO₂ and TaSiN/HfO₂ films after a 900° C/60s anneal showing TaSiN remains amorphous. (IL=interfacial layer)

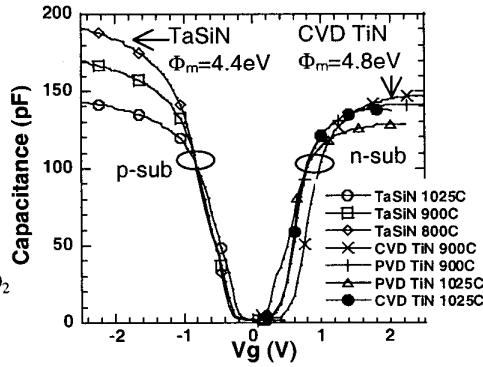


Fig. 2. CVs of n- and p-substrate HfO₂ capacitors with different metal gates and post-gate anneal temperatures. (area=1E-4 cm²)

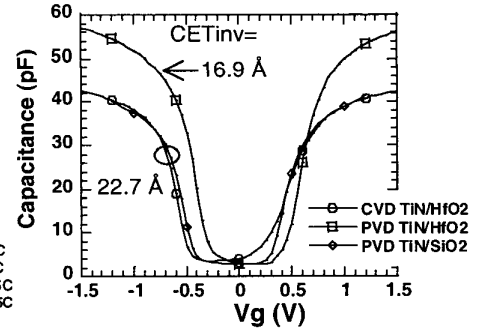


Fig. 3 High frequency CV characteristics of HfO₂ p-MOSFETs with different metal gates.

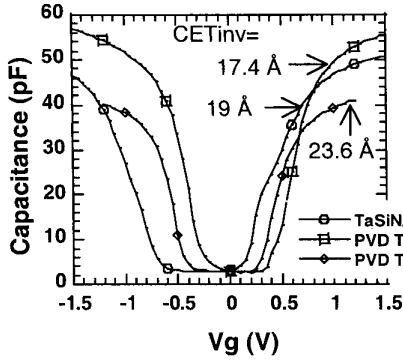


Fig. 4 High frequency CV characteristics of HfO₂ n-MOSFETs with different metal gates. (area=2.8E-5 cm² in Figs. 3 and 4)

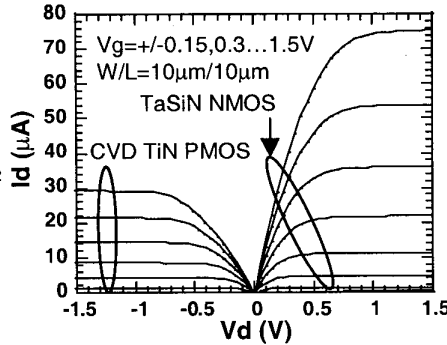


Fig. 5 Id-Vd characteristics of HfO₂ (p) n-MOSFET with (CVD TiN) TaSiN gate.

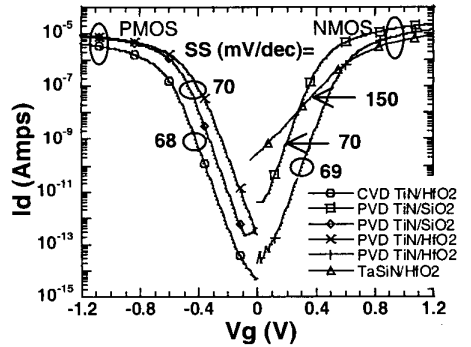


Fig. 6 Sub-threshold characteristics of 10μm x 10μm (W/L) HfO₂ n and p-MOSFETs with metal gates.

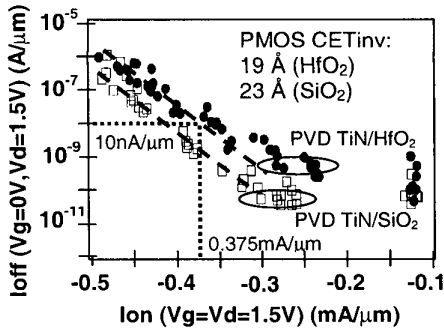


Fig. 7 PMOS Ion/Ioff data comparing HfO₂ and SiO₂ with PVD TiN gate.

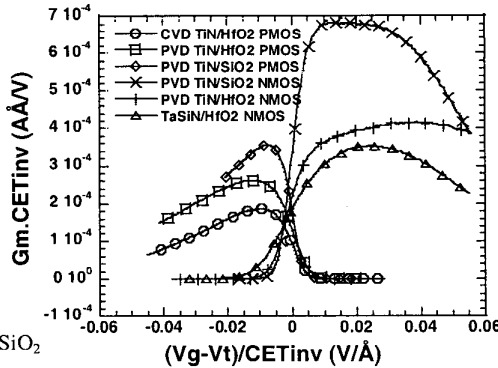


Fig. 8 PMOS and NMOS linear Gm normalized to CETinv and Vt

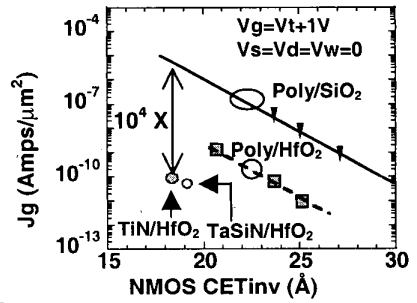


Fig. 9 NMOS gate leakage as a function of CETinv

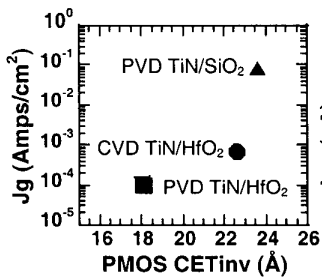


Fig. 10 PMOS gate leakage as a function of CETinv.

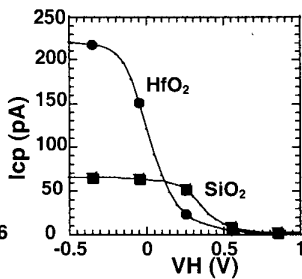


Fig. 11 Charge pumping current from SiO₂ and HfO₂ p-MOSFETs with PVD TiN gates. The current is proportional to interface trap density.

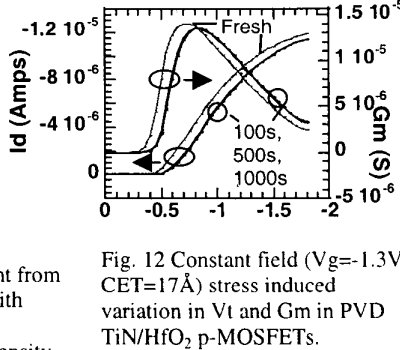


Fig. 12 Constant field (Vg=-1.3V, CET=17Å) stress induced variation in Vt and Gm in PVD TiN/HfO₂ p-MOSFETs.

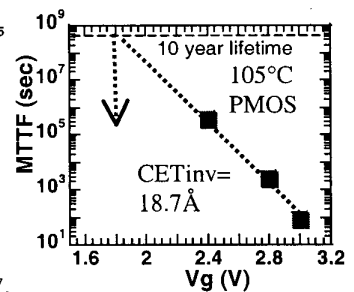


Fig. 13 TDDB data from PVD TiN/HfO₂ p-MOSFETs.